

骨髓来源的间充质干细胞移植通过 ROS/Nrf2 信号对血管性痴呆大鼠线粒体自噬的影响及其机制

孙烈乾¹, 顾梦宇¹, 杨杰², 王凯漪¹, 郭高帅^{1,3}, 张宏博^{1,3}, 张思怡^{1,3}, 王堂龙³, 杨志伟^{1,3},
贺延妮^{1,3}, 杨超^{1,3}

(1. 湖北中医药大学第一临床学院, 湖北 武汉 430065; 2. 湖北省中医院肿瘤科, 湖北 武汉 430061;
3. 湖北省中西医结合医院老年病科, 湖北 武汉 430015)

[摘要] **目的:** 探讨骨髓来源的间充质干细胞 (BMSCs) 移植通过活性氧 (ROS) /核因子 E2 相关因子 2 (Nrf2) 信号对血管性痴呆 (VaD) 大鼠线粒体自噬的影响, 并阐明其作用机制。**方法:** 将 45 只 SD 雄性成年大鼠随机分为假手术组、模型组、空载组、BMSCs 组和 BMSCs+ML385 (Nrf2 抑制剂) 组 (联合组), 每组 9 只。各组大鼠腹腔注射麻醉后, 除假手术组外, 其余各组大鼠制备 VaD 模型。采用 Morris 水迷宫实验检测各组大鼠的学习记忆能力, HE 染色观察各组大鼠脑组织病理形态表现, 尼氏染色观察各组大鼠脑组织海马区尼氏体变化情况, 透射电镜观察各组大鼠脑组织海马区超微结构, 荧光探针法检测各组大鼠脑组织海马区神经元中 ROS 水平, Western blotting 法检测各组大鼠脑组织中 Nrf2、血红素加氧酶 1 (HO-1)、磷酸酶与张力蛋白同源物诱导激酶 1 (PINK1)、E3 泛素蛋白连接酶 parkin (Parkin)、苯氯素 1 (Beclin-1) 和泛素结合蛋白 P62 (P62) 蛋白表达水平及微管相关蛋白 1A/1B 轻链 3 (LC3-II/LC3-I) 比值。**结果:** Morris 水迷宫实验, 与假手术组比较, 模型组大鼠逃避潜伏期明显延长 ($P<0.01$), 穿越原平台次数和停留时间均明显减少 ($P<0.01$); 与模型组比较, BMSCs 组大鼠逃避潜伏期明显缩短 ($P<0.01$), 穿越原平台次数和停留时间均明显增加 ($P<0.01$); 与 BMSCs 组比较, 联合组大鼠逃避潜伏期明显延长 ($P<0.01$), 穿越原平台次数和停留时间均明显减少 ($P<0.01$)。HE 染色观察, 假手术组大鼠脑组织海马区神经元数量和形态正常, 染色均匀, 结构清晰, 未见明显病变; 与假手术组比较, 模型组大鼠脑组织海马区组织稀疏, 结构紊乱, 神经元数量减少且形态不一, 染色不均匀, 核固缩, 可见部分坏死的神经元; 与模型组比较, 空载组大鼠脑组织海马区可见组织结构紊乱、神经元减少和染色不均等损伤表现, BMSCs 组大鼠海马区神经元损伤减轻, 形态恢复正常, 排列较为整齐, 神经元丢失情况明显改善; 与 BMSCs 组比较, 联合组大鼠海马区神经元形态不规则, 组织结构紊乱, 细胞边界不清, 染色不均匀, 核固缩。尼氏染色观察, 假手术组大鼠脑组织海马区神经元排列整齐紧密, 形态规则完整, 核仁明显, 尼氏小体着色深且数量多; 与假手术组比较, 模型组大鼠脑组织海马区神经元固缩, 呈空泡状, 尼氏小体着色少且数量稀少; 与模型组比较, 空载组大鼠脑组织海马区可见尼氏小体着色少且数量稀少等损伤表现, BMSCs 组大鼠脑组织海马区神经元固缩减少, 细胞形态相对完整, 尼氏小体数量相对增多; 与 BMSCs 组比较, 联合组大鼠脑组织神经元固缩, 形态完整性丧失, 尼氏小体破碎且数量减少。透射电镜观察, 假手术组大鼠脑组织海马区神经元线粒体呈椭圆形, 双层膜结构清晰可见, 内部嵴完整; 与假手术组比较, 模型组

[收稿日期] 2024-06-20 [录用日期] 2024-09-14

[基金项目] 湖北省卫健委卫生健康科研项目 (WJ2023M097); 湖北省科技厅自然科学基金项目 (2023AFB914); 湖北省中医药管理局青年人才项目 (ZY2023Q010); 湖北省中西医结合医院“杏林人才工程”青年项目 (H2023Q009); 湖北省鄂州市科技局基础人才与创新专项 (EZ01-007-20230100)

[作者简介] 孙烈乾 (2001—), 男, 湖北省荆州市人, 在读硕士研究生, 主要从事中西医结合防治老年病方面的研究。

[通信作者] 杨超, 副主任医师, 硕士研究生导师 (E-mail: yc250820883@163.com)

©《吉林大学学报 (医学版)》编辑部, 开放获取遵循 CC BY-NC-ND 协议。

© Editorial Board of Journal of Jilin University (Medicine Edition). Open access under CC BY-NC-ND license.

大鼠脑组织海马区神经元线粒体肿胀变形, 双层膜结构破坏, 内部嵴断裂消失, 结构模糊, 胞质中可见大量自噬小体; 与模型组比较, 空载组大鼠脑组织海马区线粒体损伤表现仍较明显, 胞质中自噬小体数量较多, BMSCs组大鼠脑组织海马区神经元线粒体膜和内部结构有明显改善, 损伤程度减轻, 胞质中可见少量自噬小体; 与BMSCs组比较, 联合组大鼠脑组织海马区神经元线粒体肿胀, 双层膜结构破坏, 内部嵴断裂消失, 胞质中可见自噬小体。荧光探针法, 与假手术组比较, 模型组大鼠脑组织海马区神经元中ROS水平明显升高 ($P<0.01$); 与模型组比较, BMSCs组大鼠脑组织海马区神经元中ROS水平明显降低 ($P<0.01$); 与BMSCs组比较, 联合组大鼠脑组织海马区神经元中ROS水平明显升高 ($P<0.01$)。Western blotting法, 与假手术组比较, 模型组大鼠脑组织中Nrf2和HO-1蛋白表达水平明显降低 ($P<0.01$); 与模型组比较, BMSCs组大鼠脑组织中Nrf2和HO-1蛋白表达水平明显升高 ($P<0.01$); 与BMSCs组比较, 联合组大鼠脑组织中Nrf2和HO-1蛋白表达水平明显降低 ($P<0.01$)。与假手术组比较, 模型组大鼠脑组织中Parkin、PINK1和Beclin-1蛋白表达水平及LC3-II/LC3-I比值均明显升高 ($P<0.01$), P62蛋白表达水平明显降低 ($P<0.01$); 与模型组比较, BMSCs组大鼠脑组织中Parkin、PINK1和Beclin-1蛋白表达水平及LC3-II/LC3-I比值均明显降低 ($P<0.01$), P62蛋白表达水平明显升高 ($P<0.01$); 与BMSCs组比较, 联合组大鼠脑组织中Parkin、PINK1和Beclin-1蛋白表达水平及LC3-II/LC3-I比值均明显升高 ($P<0.01$), P62蛋白表达水平明显降低 ($P<0.01$)。结论: BMSCs可以减轻大鼠脑组织海马区神经元病理改变, 改善VaD大鼠的认知功能, 其作用机制可能与调控ROS/Nrf2信号通路抑制线粒体自噬有关。

[关键词] 血管性痴呆; 骨髓来源的间充质干细胞; 核因子E2相关因子2; 活性氧; 线粒体自噬

[中图分类号] R743.9 [文献标志码] A

Effect of bone marrow-derived mesenchymal stem cell transplantation on mitochondrial autophagy in rats with vascular dementia through ROS/Nrf2 signaling and its mechanism

SUN Lieqian¹, GU Mengyu¹, YANG Jie², WANG Kaiyi¹, GUO Gaoshuai^{1,3}, ZHANG Hongbo^{1,3}, ZHANG Siyi^{1,3}, WANG Tanglong³, YANG Zhiwei^{1,3}, HE Yanni^{1,3}, YANG Chao^{1,3}

(1. First Clinical Medical College, Hubei University of Chinese Medicine, Wuhan 430065, China;

2. Department of Oncology, Hubei Provincial Hospital of Integrated Chinese and Western Medicine,

Wuhan 430061, China; 3. Department of Geriatrics, Hubei Provincial Hospital of Traditional Chinese Medicine, Wuhan 430015, China)

ABSTRACT Objective: To discuss the effects of bone marrow-derived mesenchymal stem cells (BMSCs) transplantation on mitophagy in the vascular dementia (VaD) rats through reactive oxygen species (ROS)/nuclear factor erythroid 2-related factor 2 (Nrf2) signaling, and to clarify its mechanism. **Methods:** Forty-five male adult SD rats were randomly divided into sham operation group, model group, unloaded group, BMSCs group, and MSCs+ML385 (Nrf2 inhibitor) group (combination group), and there were 9 rats in each group. After intraperitoneal anesthesia, the VaD models were established in all groups except sham operation group. Morris water maze test was used to detect the learning and memory abilities of the rats in various groups; HE staining was used to observe the histopathological morphology of brain tissue of the rats in various groups; Nissl staining was used to observe the changes of Nissl bodies in hippocampus region of brain tissue of the rats in various groups; transmission electron microscope was used to observe the ultrastructure of hippocampus region of the rats in various groups; fluorescence probe method was used to

detect the ROS levels in hippocampus neurons in various groups; Western blotting method was used to detect the expression levels of Nrf2, heme oxygenase-1 (HO-1), PTEN-induced putative kinase 1 (PINK1), parkin RBR E3 ubiquitin protein ligase (Parkin), Beclin-1, ubiquitin-binding protein p62 (P62), and microtubule-associated protein 1A/1B-light chain 3 (LC3-II/LC3-I) ratio in brain tissue of the rats in various groups. **Results:** The Morris water maze results showed that compared with sham operation group, the escape latency of the rats in model group was significantly increased ($P < 0.01$), while the number of crossing time and residence time were significantly decreased ($P < 0.01$). Compared with model group, the escape latency of the rats in BMSCs group was significantly decreased ($P < 0.01$), while the number of crossing time and residence time were significantly increased ($P < 0.01$). Compared with BMSCs group, the escape latency of the rats in combination group was significantly increased ($P < 0.01$), while the number of crossing time and residence time were significantly decreased ($P < 0.01$). The HE staining results showed that hippocampus neurons of the rats in sham operation group were normal in quantity and morphology, with uniform staining and clear structure. Compared with sham operation group, the hippocampus tissue of the rats in model group showed sparse arrangement, disordered structure, reduced neuronal quantity, varied morphology, uneven staining, nuclear pyknosis, and partial neuronal necrosis. Compared with model group, the neuronal damage of the rats in hippocampus regio in BMSCs group was alleviated, with restored morphology and improved neuronal loss. Compared with BMSCs group, the neurons of the rats in hippocampus region in combination group showed irregular morphology, disordered structure, unclear cell boundaries, uneven staining, and nuclear pyknosis. The Nissl staining results showed that the hippocampal neurons in sham operation group were tightly arranged with intact morphology, obvious nucleoli, and abundant darkly stained Nissl bodies. Compared with sham operation group, the neurons in hippocampus region of the rats in model group showed pyknosis, vacuolization, and sparse Nissl bodies. Compared with model group, the BMSCs group showed reduced neuronal pyknosis, relatively intact morphology, and increased Nissl bodies. Compared with BMSCs group, the combination group showed neuronal pyknosis, loss of morphological integrity, and fragmented Nissl bodies. The transmission electron microscope results showed that mitochondria in sham operation group exhibited oval shape with intact double-membrane structure and cristae. Compared with sham operation group, the mitochondria in model group showed swelling, disrupted membranes, broken cristae, and numerous autophagosomes. Compared with model group, the BMSCs group showed improved mitochondrial structure and reduced autophagosomes. Compared with BMSCs group, the combination group showed swollen mitochondria, disrupted membranes, broken cristae, and visible autophagosomes. The fluorescence probe results showed that compared with sham operation group, the ROS levels in the hippocampus neurons in brain tissue of the rats in model group were significantly increased ($P < 0.01$); compared with model group, the ROS levels in hippocampus neurons in brain tissue of the rats in BMSCs group were significantly decreased ($P < 0.01$); compared with BMSCs group, the ROS levels in hippocampus neurons in brain tissue of the rats in combination group were significantly increased ($P < 0.01$). The Western blotting results showed that compared with sham operation group, the expression levels of Nrf2 and HO-1 proteins in brain tissue of the rats in model group were significantly decreased ($P < 0.01$); compared with model group, the expression levels of Nrf2 and HO-1 proteins in brain tissue of the rats in BMSCs group were significantly increased ($P < 0.01$); compared with BMSCs group, the expression levels of Nrf2 and HO-1 proteins in brain tissue of the rats in combination group were significantly decreased ($P < 0.01$); compared with sham operation group, the expression levels of Parkin, PINK1, and Beclin-1 proteins, and LC3-II/LC3-I ratio of the rats in model group were significantly increased ($P < 0.01$), while the expression level of P62 protein was significantly decreased ($P < 0.01$); compared with model group, the expression levels of Parkin, PINK1, and Beclin-1 proteins, as well as the LC3-II/LC3-I ratio, of the rats in BMSCs

group were significantly decreased ($P < 0.01$), while the expression level of P62 protein was significantly increased ($P < 0.01$); compared with BMSCs group, the expression levels of Parkin, PINK1, and Beclin-1 proteins, as well as the LC3-II/LC3-I ratio, of the rats in combination group were significantly increased ($P < 0.01$), while the expression level of P62 protein was significantly decreased ($P < 0.01$).

Conclusion: BMSCs can alleviate the hippocampal neuronal pathological changes and improve cognitive function in the VaD rats, and its mechanism may be related to the regulation of ROS/Nrf2 signaling pathway to inhibit mitophagy.

KEYWORDS Vascular dementia; Bone marrow mesenchymal stem cells; Nuclear factor erythroid 2-related factor 2; Reactive oxygen species; Mitophagy

血管性痴呆 (vascular dementia, VaD) 是一种获得性智能障碍综合征, 由各种脑血管疾病引起脑功能障碍, 属于血管性认知障碍^[1]。VaD 是最常见的老年期痴呆疾病之一, 发病率随着年龄的增加而升高, 患病人数占全部老年痴呆人数的 15%~20%, 仅次于阿尔茨海默病^[2-4]。VaD 的主要病理改变为脑血管损伤导致的脑组织病变, 如多发性皮层和皮层下梗死等, 主要临床表现为认知和行为障碍。随着疾病的进展, 相关症状也逐渐加重, 对患者的生活质量产生严重影响, 并给家庭、社会和医疗保健系统造成巨大的压力^[5-6]。因此, 明确 VaD 的发生发展机制并寻找有效的干预手段对于 VaD 的治疗具有重要意义。

在正常条件下, 神经元内的失能线粒体会通过自噬清除, 以维持正常的能量代谢和细胞内环境的稳态^[7]。本课题组前期研究^[8]和相关研究^[9]结果显示: VaD 发生时, 神经元处于氧化应激状态, 活性氧 (reactive oxygen species, ROS) 大量产生, ROS 水平升高对线粒体有害, 并通过多种机制扩散至周围线粒体, 使细胞广泛产生损伤性氧化应激, 导致线粒体自噬的广泛发生。解除该状态可抑制自噬进而改善神经组织损伤^[10]。

间充质干细胞 (mesenchymal stem cells, MSCs) 具有可进行自体移植和组织来源丰富等优势^[11]。研究^[12-13]表明: MSCs 通过分泌细胞因子和释放细胞外囊泡等方式, 塑造有利于组织修复的微环境, 从而促进损伤修复。MSCs 还能够减少氧化损伤, 并通过抑制细胞凋亡提高受损组织细胞的存活率^[14-16]。MSCs 还可通过调节神经元自噬水平改善神经元凋亡, 显示出潜在的神经保护作用^[17]。然而, 其在神经系统疾病中的具体作用机制仍需进一步探讨。

目前, MSCs 通过调节氧化应激及线粒体自噬改善 VaD 的认知状态及其修复作用机制的研究较少。本研究使用骨髓来源的间充质干细胞 (bone

marrow-derived MSCs, BMSCs), 通过尾静脉注射至 VaD 模型大鼠体内, 观察其对 VaD 大鼠的治疗作用, 并评估 BMSCs 对大鼠海马神经元氧化应激状态及线粒体自噬的调控情况, 旨在为 VaD 的研究提供新的思路。

1 材料与方法

1.1 实验动物、细胞、主要试剂及仪器 8~10 周龄雄性 SPF 级 SD 大鼠 45 只, 体质量 (300±40) g, 购自长沙市天勤生物技术有限公司, 动物生产许可证号: SCXK (湘) 2022-0011。大鼠饲养于清洁级动物房, 环境温度保持在 20℃~24℃, 相对湿度为 50%~70%, 每日 12 h 明暗交替, 自由进食和饮水, 适应性饲养 1 周后进行实验。本研究获得湖北省中西医结合医院伦理委员会批准, 伦理审批号: (2023) 伦审第 (研 002) 号。所有参与实验的人员均通过湖北省实验动物从业人员专业技术考试并取得合格证书, 实验过程严格遵循 3R 原则及动物福利相关规定, 并给予实验动物人道关怀。大鼠 BMSCs 购自赛业生物科技有限公司。核因子 E2 相关因子 2 (nuclear factor erythroid 2-related factor, Nrf2) 抑制剂 ML385 (美国 MedChemExpress 公司), HE 染色试剂盒 (北京索莱宝科技有限公司), 尼氏染液 (武汉四维加生物科技有限公司), RIPA 裂解液 (上海碧云天生物科技有限公司), BCA 蛋白浓度测定试剂盒 (美国赛默飞世尔科技公司), ECL 化学发光试剂盒 (北京兰杰柯科技有限公司), 二氢乙锭 (Dihydroethidium, DHE) 和 4', 6-二脒基-2-苯基吲哚 (4', 6-diamidino-2-phenylindole, DAPI) 染色液 (美国 Sigma 公司), 抗荧光淬灭封片剂 (美国 Southern Biotech 公司), 磷酸酶与张力蛋白同源物诱导激酶 1 (phosphatase and tensin homolog induced putative kinase 1, PINK1) 抗体、E3 泛素蛋白连接酶 parkin (E3

ubiquitin-protein ligase parkin, Parkin) 抗体、血红素加氧酶1 (heme oxygenase-1, HO-1) 抗体、泛素结合蛋白 P62 (ubiquitin-binding protein P62, P62) 抗体、苜蓿素1 (Beclin-1) 抗体和微管相关蛋白1A/1B轻链3 (microtubule-associated proteins 1A/1B light chain 3, LC3) 抗体(美国Abclonal公司), Nrf2抗体(武汉三鹰生物技术有限公司)。Morris水迷宫视频分析系统(型号: SA20, 江苏赛昂斯生物科技有限公司), 病理切片机(型号: RM2016)、超薄切片机(型号: LEICA UC7) 和正置荧光显微镜(型号: LEICA DM2000LED) 均购自德国LEICA公司, 透射电镜(型号: JEM-1400, 日本电子株式会社), 冰冻切片机(型号: CRYOSTAR NX50, 美国赛默飞世尔科技公司), 扫描仪(型号: Panoramic MIDI, 匈牙利3DHISTECH公司), 电泳槽(型号: DYCZ-24, 北京六一生物技术有限公司)。

1.2 实验动物造模、分组及给药 45只SD大鼠适应性喂养7 d后随机分为假手术组、模型组、空载组、BMSCs组和BMSCs+ML385组(联合组), 每组9只。各组大鼠腹腔注射麻醉后, 除假手术组外, 其余各组大鼠行双侧颈总动脉分次结扎手术, 制备VaD模型(改良2VO模型)。手术过程中, 各组大鼠经碘伏消毒皮肤后沿颈正中中线切开, 分离周围组织, 暴露右侧颈总动脉, 并在近心端及远心端结扎后切断。逐层缝合皮肤及肌肉, 待苏醒后正常喂养。1周后, 以相同方式结扎并切断左侧颈总动脉, 完成造模。假手术组大鼠仅暴露双侧颈总动脉后立即缝合, 其他操作同上。造模成功7 d后, 将BMSCs以 $2 \times 10^6 \text{ mL}^{-1}$ 的细胞密度通过尾静脉注射1 mL至BMSCs组和联合组大鼠体内; 假手术组和模型组大鼠则以相同方式注射1 mL生理盐水; 空载组大鼠通过尾静脉注射1 mL磷酸盐缓冲液(phosphate buffer saline, PBS)。联合组大鼠将ML385溶于含5%二甲基亚砜(dimethyl sulfoxide, DMSO)的PBS缓冲液中, 在BMSCs移植前3 d开始注射($30 \text{ mg} \cdot \text{kg}^{-1}$), 持续7 d, 其余组大鼠均以相同方式接受等量含5% DMSO的PBS缓冲液。Morris水迷宫实验测试结束后处死大鼠取脑组织, 将部分脑组织置于4%多聚甲醛中固定, 其余组织液氮速冻后储存于 -80°C 冰箱中备用。

1.3 Morris水迷宫实验检测各组大鼠学习记忆能力 第1~5天为定位航行实验, 确定第一至第

四象限位置, 将逃生平台置于第四象限, 第1天水面低于平台1 cm, 第2~5天水面没过平台。按相同顺序依次从4个象限中点将大鼠放入水中, 记录各组大鼠寻找平台时间, 每次时间限制为120 s, 若大鼠在120 s内找到平台并停留3 s以上, 则认为大鼠找到平台, 记录该时间为逃避潜伏期; 若120 s内未找到平台则诱导其在平台上站立10 s。第6天进行空间探索实验, 检测大鼠学习记忆能力。撤去原平台, 将大鼠从各象限中点放入水中, 记录大鼠120 s内穿越原平台区域次数和目标象限停留时间。

1.4 HE染色观察各组大鼠脑组织病理形态表现

各组大鼠脑组织置于4%多聚甲醛中固定, 常规石蜡包埋、切片。石蜡切为 $4 \mu\text{m}$ 薄片, 二甲苯透明, 梯度乙醇水化, 采用HE染色试剂盒染色, 脱水透明封片, 于显微镜下观察各组大鼠脑组织病理形态表现。

1.5 尼氏染色观察各组大鼠脑组织海马区尼氏体变化情况

制作石蜡组织切片过程同“1.4”。石蜡切片经尼氏染液染色2~5 min, 蒸馏水稍洗, 根据组织着色深浅用0.1%冰醋酸对切片进行分化, 置入 65°C 烤箱中烘干, 中性树胶封片, 显微镜下观察各组大鼠脑组织尼氏体变化情况。

1.6 透射电镜观察各组大鼠脑组织海马区超微结构

取 1 mm^3 大小新鲜海马组织, 迅速投入电镜固定液中 4°C 固定4 h。PBS缓冲液漂洗3次后, 1%锇酸 20°C 固定2 h, PBS缓冲液漂洗3次后乙醇梯度脱水, 使用丙酮及812包埋剂包埋, 采用超薄切片机进行切片, 2%醋酸铀饱和水溶液及枸橼酸铅双染色, 透射电镜观察各组大鼠脑组织海马区超微结构。

1.7 荧光探针法检测各组大鼠脑组织海马区神经元中ROS水平

将大鼠脑组织制成冰冻切片, 实验前将切片置于室温平衡30 min, PBS缓冲液洗涤3次, 滴加DHE探针, 室温下避光孵育30 min, PBS缓冲液洗涤3次, 每次5 min, DAPI染色液室温避光孵育10 min, PBS缓冲液洗涤3次, 每次5 min, 抗荧光淬灭封片剂封片, 荧光显微镜观察并拍照。采用Image J软件分析荧光强度, 以荧光强度代表ROS水平。

1.8 Western blotting法检测各组大鼠脑组织海马区中Nrf2、HO-1、PINK1、Parkin、Beclin-1和P62蛋白表达水平及LC3-II/LC3-I比值

将冻存的大鼠

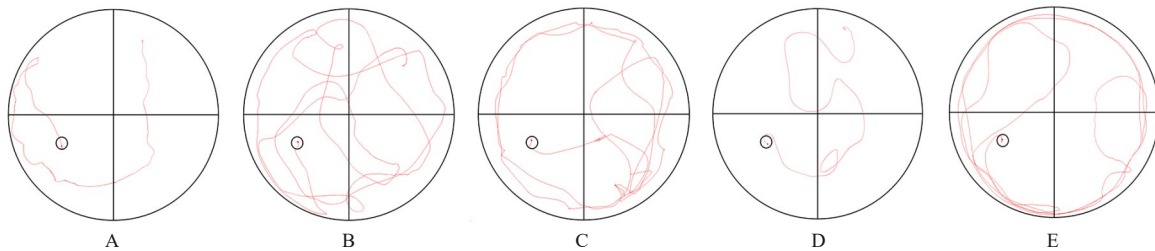
脑组织海马区取出, 添加适量 RIPA 裂解液匀浆, 静置 30 min。4 °C、12 000 r·min⁻¹ 离心 15 min 吸取上清液, BCA 法检测蛋白浓度并加入上样缓冲液, 加热 10 min 使蛋白变性。取 SDS-PAGE 凝胶上样并开启电泳分离蛋白, 并转移至 PVDF 膜。转膜完毕后, 以 5% 脱脂奶粉作为封闭液, 置于摇床中缓慢摇动, 室温封闭 1 h。参照一抗说明书配制一抗稀释液, 4 °C 孵育过夜。TBST 溶液洗涤 3 次, 每次 5 min, 参照二抗说明书配制二抗稀释液, 室温孵育 1 h, TBST 溶液洗涤 3 次, 每次 5 min, ECL 化学发光剂显影, 采用 Image J 软件分析蛋白条带灰度值, 以 β -actin 为内参, 计算目的蛋白表达水平。目的蛋白表达水平 = 目的蛋白条带灰度值 / 内参蛋白条带灰度值。

1.9 统计学分析 采用 SPSS 23.0 统计软件进行统计学分析。各组大鼠逃避潜伏期、穿越平台次数、原平台停留时间, 脑组织中 ROS 水平和 Nrf2、

HO-1、PINK1、Parkin、P62 及 Beclin-1 蛋白表达水平以及 LC3-II / LC3-I 比值均符合正态分布, 以 $\bar{x} \pm s$ 表示, 多组间样本均数比较采用单因素方差分析, 组间样本均数两两比较采用 LSD-*t* 检验。以 $P < 0.05$ 为差异有统计学意义。

2 结果

2.1 各组大鼠逃避潜伏期、穿越原平台次数和停留时间 与假手术组比较, 模型组大鼠逃避潜伏期明显延长 ($P < 0.01$), 穿越原平台次数和停留时间均明显减少 ($P < 0.01$); 与模型组比较, BMSCs 组大鼠逃避潜伏期明显缩短 ($P < 0.01$), 穿越原平台次数和停留时间均明显增加 ($P < 0.01$), 空载组大鼠逃避潜伏期、穿越原平台次数和停留时间差异均无统计学意义 ($P > 0.05$); 与 BMSCs 组比较, 联合组大鼠逃避潜伏期明显延长 ($P < 0.01$), 穿越原平台次数和停留时间均明显减少 ($P < 0.01$)。见图 1 和表 1。



A: Sham operation group; B: Model group; C: Unloaded group; D: BMSCs group; E: Combination group.

图 1 各组大鼠 Morris 水迷宫轨迹图

Fig. 1 Morris water maze track diagrams of rats in various groups

表 1 各组大鼠逃避潜伏期、穿越原平台次数和停留时间

Tab. 1 Escape latency, number of crossing time, and residence time in platform quadrant of rats in various groups

($n=9, \bar{x} \pm s$)

Group	Escape latency(t/s)	Number of crossing time	Residence time in platform quadrant(t/s)
Sham operation	23.61 ± 2.40	11.67 ± 2.35	58.29 ± 2.72
Model	37.60 ± 2.93*	4.00 ± 2.06*	32.87 ± 2.92*
Unloaded	37.71 ± 2.29	4.22 ± 1.79	32.67 ± 2.94
BMSCs	26.64 ± 2.40 [△]	10.44 ± 2.51 [△]	51.30 ± 4.20 [△]
Combination	36.24 ± 3.17 [#]	5.33 ± 1.50 [#]	38.83 ± 3.35 [#]

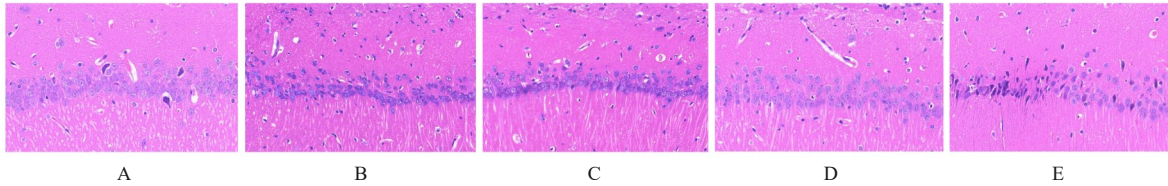
* $P < 0.01$ vs sham operation group; [△] $P < 0.01$ vs model group; [#] $P < 0.01$ vs BMSCs group.

2.2 各组大鼠脑组织病理形态表现 假手术组大鼠脑组织海马区神经元数量和形态正常, 染色均匀, 结构清晰, 未见明显病变; 与假手术组比较, 模型组大鼠脑组织海马区组织稀疏, 结构紊乱, 神经元

数量减少、形态不一, 染色不均匀, 核固缩, 可见部分坏死的神经元; 与模型组比较, 空载组大鼠脑组织海马区可见组织结构紊乱, 神经元减少及染色不均等损伤表现, BMSCs 组大鼠脑组织海马区神

神经元损伤减轻,形态恢复正常,排列较为整齐,神经元丢失情况明显改善;与BMSCs组比较,联合组

大鼠脑组织海马区神经元形态不规则,组织结构紊乱,细胞边界不清,染色不均匀,核固缩。见图2。



A: Sham operation group; B: Model group; C: Unloaded group; D: BMSCs group; E: Combination group.

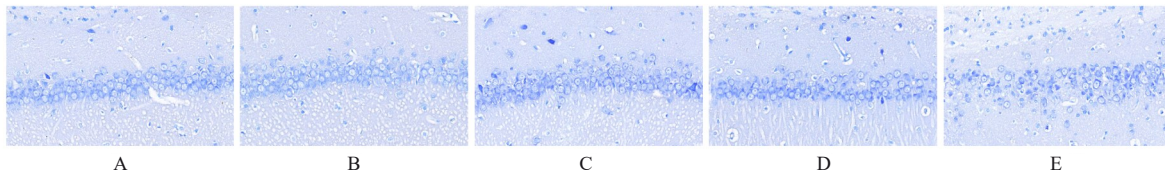
图2 HE染色观察各组大鼠脑组织病理形态表现($\times 400$)

Fig. 2 Pathomorphology of brain tissue of rats in various groups observed by HE staining ($\times 400$)

2.3 各组大鼠海马区尼氏体变化情况 假手术组大鼠脑组织海马区神经元排列整齐紧密,形态规则完整,核仁明显,尼氏小体着色深且数量多;与假手术组比较,模型组大鼠脑组织海马区神经元固缩,呈空泡状,尼氏小体着色少且数量稀少;与模型组比较,空载组大鼠脑组织海马区可见尼氏小体着色少且数量稀少等损伤表现,BMSCs组大鼠脑组织海马区神经元固缩减少,细胞形态相对完整,尼氏小体数量相对增多;与BMSCs组比较,联合组大鼠脑组织神经元固缩,形态完整性丧失,尼氏小体破碎、数量减少。见图3。

2.4 各组大鼠脑组织海马区超微结构 假手术组

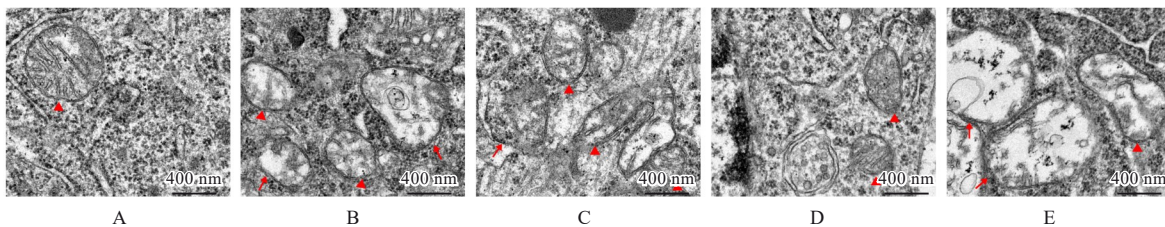
大鼠脑组织海马区神经元线粒体呈椭圆形,双层膜结构清晰可见,内部嵴完整;与假手术组比较,模型组大鼠脑组织海马区神经元线粒体肿胀变形,双层膜结构被破坏,内部嵴断裂消失,结构模糊,胞质中可见大量自噬小体;与模型组比较,空载组大鼠脑组织海马区线粒体损伤表现仍较明显,胞质中自噬小体数量较多,BMSCs组大鼠脑组织海马区神经元线粒体膜和内部结构有明显改善,损伤程度减轻,胞质中可见少量自噬小体;与BMSCs组比较,联合组大鼠脑组织海马区神经元线粒体肿胀,双层膜结构破坏,内部嵴断裂消失,胞质中可见自噬小体。见图4。



A: Sham operation group; B: Model group; C: Unloaded group; D: BMSCs group; E: Combination group.

图3 尼氏染色观察各组大鼠脑组织海马区尼氏体变化情况($\times 400$)

Fig. 3 Changes of Niss body in brain tissue of rats in various groups detected by Nissl staining ($\times 400$)



Arrows indicated autophagosomes, triangles indicated mitochondria. A: Sham operation group; B: Model group; C: Unloaded group; D: BMSCs group; E: Combination group.

图4 各组大鼠脑组织海马区神经元超微结构

Fig. 4 Ultrastructure of neurons in hippocampus region in brain tissue of rats in various groups

2.5 各组大鼠脑组织海马区神经元中 ROS 水平

与假手术组比较, 模型组大鼠脑组织海马区神经元中 ROS 水平明显升高 ($P < 0.01$); 与模型组比较, BMSCs 组大鼠脑组织海马区神经元中 ROS 水平明

显降低 ($P < 0.01$), 空载组大鼠脑组织海马区 ROS 水平差异无统计学意义 ($P > 0.05$); 与 BMSCs 组比较, 联合组大鼠脑组织海马区神经元中 ROS 水平明显升高 ($P < 0.01$)。见图 5 和表 2。

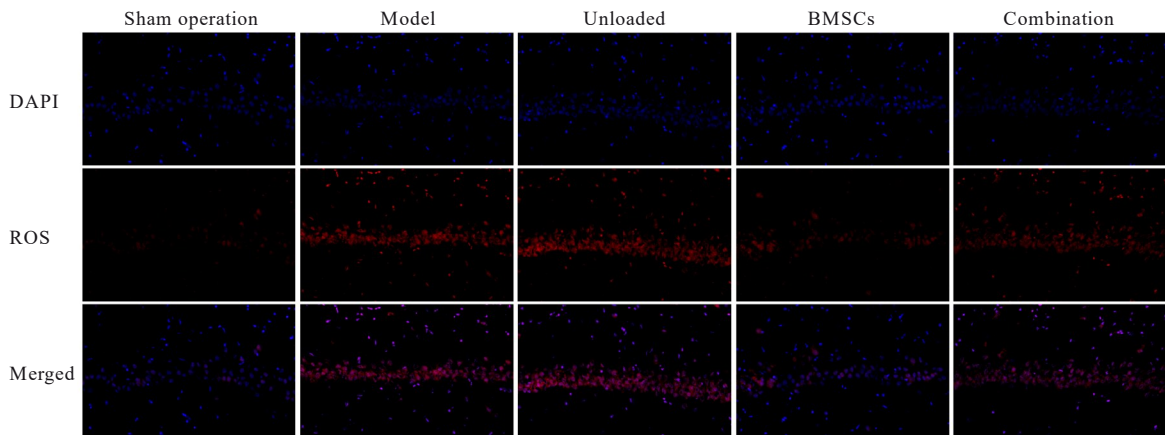


图 5 各组大鼠脑组织海马区神经元 ROS 表达情况 ($\times 800$)

Fig. 5 Expressions of ROS in neurons in hippocampus region in brain tissue of rats in various groups ($\times 800$)

表 2 各组大鼠脑组织海马区神经元 ROS 水平

Tab. 2 ROS levels in neurons in hippocampus region in brain tissue of rats in various groups ($n=3, \bar{x} \pm s$)

Group	Level of ROS
Sham operation	30.89 ± 2.96
Model	$87.77 \pm 2.06^*$
Unloaded	84.10 ± 2.69
BMSCs	$42.87 \pm 3.35^\Delta$
Combination	$69.17 \pm 4.18^\#$

* $P < 0.01$ vs sham operation group; $^\Delta P < 0.01$ vs model group; $^\# P < 0.01$ vs BMSCs group.

2.6 各组大鼠脑组织中 Nrf2 和 HO-1 蛋白表达水平

与假手术组比较, 模型组大鼠脑组织中 Nrf2 和 HO-1 蛋白表达水平均明显降低 ($P < 0.01$); 与模型组比较, BMSCs 组大鼠脑组织中 Nrf2 和 HO-1 蛋白表达水平均明显升高 ($P < 0.01$), 空载组大鼠脑组织中 Nrf2 和 HO-1 蛋白表达水平差异均无统计学意义 ($P > 0.05$); 与 BMSCs 组比较, 联合组大鼠脑组织中 Nrf2 和 HO-1 蛋白表达水平均明显降低 ($P < 0.01$)。见图 6。

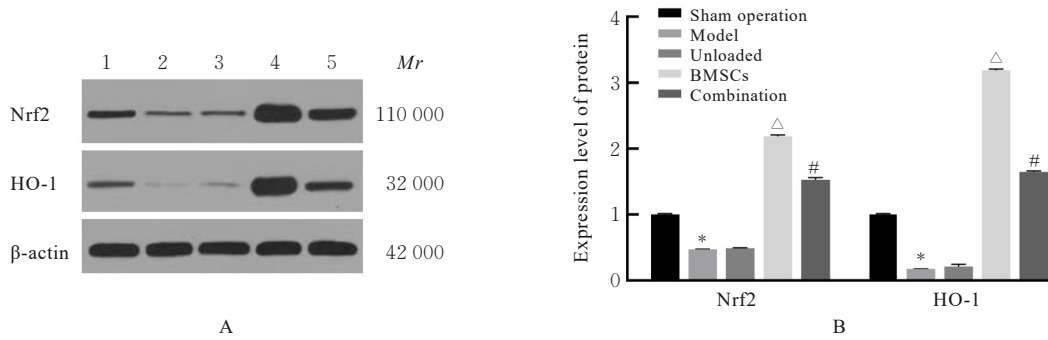
2.7 各组大鼠脑组织中 Parkin、PINK1、P62 和 Beclin-1 蛋白表达水平及 LC3-II/LC3-I 比值 与假手术组比较, 模型组大鼠脑组织中 Parkin、PINK1 和 Beclin-1 蛋白表达水平及 LC3-II/LC3-I 比值均明显升高 ($P < 0.01$), P62 蛋白表达水平明

显降低 ($P < 0.01$); 与模型组比较, BMSCs 组大鼠脑组织中 Parkin、PINK1 和 Beclin-1 蛋白表达水平及 LC3-II/LC3-I 比值均明显降低 ($P < 0.01$), P62 蛋白表达水平明显升高 ($P < 0.01$), 空载组大鼠脑组织中 Parkin、PINK1 和 Beclin-1 和 P62 蛋白表达水平及 LC3-II/LC3-I 比值差异均无统计学意义 ($P > 0.05$); 与 BMSCs 组比较, 联合组大鼠脑组织中 Parkin、PINK1 和 Beclin-1 蛋白表达水平及 LC3-II/LC3-I 比值均明显升高 ($P < 0.01$), P62 蛋白表达水平明显降低 ($P < 0.01$)。见图 7。

3 讨论

VaD 是与年龄相关的、由脑血流灌注不足所致缺血缺氧或血管病变引起的认知和记忆功能障碍, 是临床常见的老年疾病^[18]。其致病机制尚未明确, 主要包括胆碱能系统的损伤、神经炎症、自由基的毒性和突触可塑性等^[2, 19]。氧化应激是各种病理过程的主要体征之一, ROS 过量产生会进一步加重脑血管和神经退行性疾病的脑组织损伤^[20]。

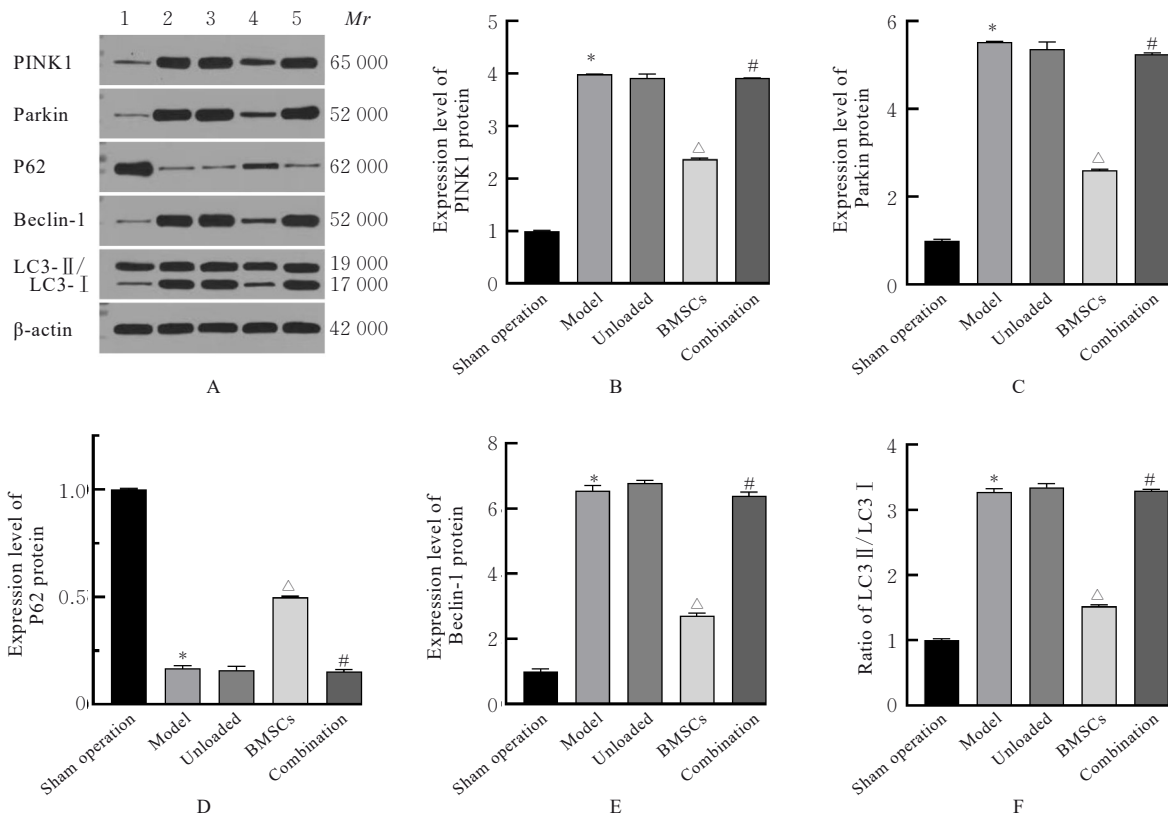
当细胞处于应激状态时, 如缺血缺氧、氧化应激反应增强、ROS 过量生成或自噬破坏等, 会激活 Nrf2^[21]。激活的 Nrf2 在细胞核中积累, 调节靶基因的转录及编码并参与抗氧化剂的合成、解毒、代谢和炎症等过程^[22-23]。本研究结果显示: 与假手术组比较, 模型组大鼠脑组织中 Nrf2 和 HO-1 蛋白表达水平降低, ROS 水平明显升高。提示 VaD 大



Lane 1: Sham operation group; Lane 2: Model group; Lane 3: Unloaded group; Lane 4: BMSCs group; Lane 5: Combination group.
* $P < 0.01$ vs sham operation group; $\Delta P < 0.01$ vs model group; # $P < 0.01$ vs BMSCs group.

图6 Western blotting法检测各组大鼠海马组织中Nrf2和HO-1蛋白表达电泳图(A)及直条图(B)

Fig. 6 Electrophoregram(A) and histogram(B) of expressions of Nrf2 and HO-1 proteins in hippocampus tissue of rats in various groups detected by Western blotting method



Lane 1: Sham operation group; Lane 2: Model group; Lane 3: Unloaded group; Lane 4: BMSCs group; Lane 5: Combination group.
* $P < 0.01$ vs sham operation group; $\Delta P < 0.01$ vs model group; # $P < 0.01$ vs BMSCs group.

图7 Western blotting法检测各组大鼠海马组织中线粒体自噬相关蛋白表达电泳图(A)及直条图(B-F)

Fig. 7 Electrophoregram(A) and histograms(B-F) of expressions of mitochondrial autophagy-related proteins in hippocampus tissue of rats in various groups detected by Western blotting method

鼠海马神经元的Nrf2调节途径受损, ROS无法及时清除, 导致受损神经元氧化应激状态无法调节。

当神经元处于氧化应激状态时, 线粒体产生大量ROS, 其通过线粒体通透性过渡孔(mitochondrial permeability transition pore, mPTP)

进入胞质内, 引起大量线粒体发生非特异性自噬, 细胞能量合成功能受损, 引起神经元凋亡^[9]。作为VaD发生发展的重要机制, 过度的线粒体自噬会导致神经元正常功能的丧失^[24]。本研究结果显示: 与假手术组比较, 模型组大鼠脑组织中线粒体自噬

相关蛋白表达上调, 海马神经元超微结构显示线粒体损伤严重, 自噬小体明显增多。

研究^[14, 25]显示: MSCs对认知障碍起重要作用, 还能够调节神经元的氧化应激状态。增强 Nrf2 活性可以减轻缺血后神经认知障碍及氧化应激状态, 缓解神经元自噬^[26-27]。因此, 经 ROS/Nrf2 信号改善神经元氧化应激状态, 调控线粒体自噬可能是 BMSCs 治疗血管性痴呆的有效靶点。

本研究中 BMSCs 干预后 Nrf2 和 HO-1 蛋白表达水平明显升高, ROS 水平降低, 线粒体自噬相关蛋白被抑制, 线粒体损伤和超微结构得到明显改善, 且大鼠脑组织海马区神经元损伤和病理变化得到明显改善。本研究中 Morris 水迷宫实验检测结果显示: BMSCs 对 VaD 大鼠空间学习能力具有保护作用。Nrf2 抑制剂部分逆转了 BMSCs 的对 VaD 模型大鼠的调节效果。提示 BMSCs 可能通过调节 ROS/Nrf2 信号通路抑制线粒体自噬减轻海马神经元损伤, 进而改善 VaD 大鼠认知功能。

综上所述, BMSCs 通过调控 ROS/Nrf2 信号通路改善 VaD 大鼠中的氧化应激状态, 抑制线粒体自噬, 进而减缓大鼠脑组织海马区神经元的损伤, 改善大鼠认知功能。但 MSCs 对 ROS/Nrf2 信号通路具体的调控机制尚需进一步研究。

利益冲突声明:

所有作者声明不存在利益冲突。

作者贡献声明:

孙烈乾参与实验设计、实验操作和论文撰写, 顾梦宇、杨杰、王凯漪和郭高帅参与实验指标检测、动物模型制备及取材, 张宏博、张思怡、王堂龙、杨志伟和贺延妮参与实验数据收集整理及统计学分析, 杨超参与实验设计指导和论文审校。

[参考文献]

- [1] 陈昭, 吴林, 蓝雪琳, 等. 血管性痴呆发病机制中西医研究进展[J]. 辽宁中医药大学学报, 2022, 24(1): 40-44.
- [2] RUNDEK T, TOLEA M, ARIKO T, et al. Vascular cognitive impairment (VCI) [J]. Neurotherapeutics, 2022, 19(1): 68-88.
- [3] WOLTERS F J, ARFAN IKRAM M. Epidemiology of vascular dementia [J]. Arterioscler Thromb Vasc Biol, 2019, 39(8): 1542-1549.
- [4] INOUE Y, SHUE F, BU G J, et al. Pathophysiology and probable etiology of cerebral small vessel disease in vascular dementia and Alzheimer's disease [J]. Mol Neurodegener, 2023, 18(1): 46.
- [5] PATHAN N, KHAROD M K, NAWAB S, et al. Genetic determinants of vascular dementia [J]. Can J Cardiol, 2024, 40(8): 1412-1423.
- [6] SANTOS M A O, BEZERRA L S, CORREIA C D C, et al. Neuropsychiatric symptoms in vascular dementia: epidemiologic and clinical aspects [J]. Dement Neuropsychol, 2018, 12(1): 40-44.
- [7] WANG D P, LI B W, WANG S C, et al. Engineered inhaled nanocatalytic therapy for ischemic cerebrovascular disease by inducing autophagy of abnormal mitochondria [J]. NPJ Regen Med, 2023, 8(1): 44.
- [8] 杨超, 杨佳, 刘玲. 涤痰汤对血管性痴呆大鼠海马 NOX2/ROS 通路、GSH、HO-1 表达的影响 [J]. 中国老年学杂志, 2019, 39(12): 3052-3055.
- [9] BONORA M, GIORGI C, PINTON P. Molecular mechanisms and consequences of mitochondrial permeability transition [J]. Nat Rev Mol Cell Biol, 2022, 23(4): 266-285.
- [10] HE Y Y, HE T T, LI H P, et al. Deciphering mitochondrial dysfunction: Pathophysiological mechanisms in vascular cognitive impairment [J]. Biomed Pharmacother, 2024, 174: 116428.
- [11] HE S Z, WANG Q Q, CHEN L K, et al. miR-100a-5p-enriched exosomes derived from mesenchymal stem cells enhance the anti-oxidant effect in a Parkinson's disease model via regulation of Nox4/ROS/Nrf2 signaling [J]. J Transl Med, 2023, 21(1): 747.
- [12] TURANO E, SCAMBI I, VIRLA F, et al. Extracellular vesicles from mesenchymal stem cells: towards novel therapeutic strategies for neurodegenerative diseases [J]. Int J Mol Sci, 2023, 24(3): 2917.
- [13] PALANISAMY C P, PEI J J, ALUGOJU P, et al. New strategies of neurodegenerative disease treatment with extracellular vesicles (EVs) derived from mesenchymal stem cells (MSCs) [J]. Theranostics, 2023, 13(12): 4138-4165.
- [14] TELI P, KALE V, VAIDYA A. Mesenchymal stromal cells-derived secretome protects Neuro-2a cells from oxidative stress-induced loss of neurogenesis [J]. Exp Neurol, 2022, 354: 114107.
- [15] JIANG X H, LI H F, CHEN M L, et al. Treadmill exercise exerts a synergistic effect with bone marrow mesenchymal stem cell-derived exosomes on neuronal apoptosis and synaptic-axonal remodeling [J]. Neural

- Regen Res, 2023, 18(6): 1293-1299.
- [16] RADWAN R R, MOHAMED H A. Mechanistic approach of the therapeutic potential of mesenchymal stem cells on brain damage in irradiated mice: emphasis on anti-inflammatory and anti-apoptotic effects[J]. Int J Radiat Biol, 2023, 99(9): 1463-1472.
- [17] ZHUO Y, LI W S, LU W, et al. TGF- β 1 mediates hypoxia-preconditioned olfactory mucosa mesenchymal stem cells improved neural functional recovery in Parkinson's disease models and patients[J]. Mil Med Res, 2024, 11(1): 48.
- [18] LINH T T D, HSIEH Y C, HUANG L K, et al. Clinical trials of new drugs for vascular cognitive impairment and vascular dementia[J]. Int J Mol Sci, 2022, 23(19): 11067.
- [19] TIAN Z M, JI X M, LIU J. Neuroinflammation in vascular cognitive impairment and dementia: current evidence, advances, and prospects[J]. Int J Mol Sci, 2022, 23(11): 6224.
- [20] JOMOVA K, RAPTOVA R, ALOMAR S Y, et al. Reactive oxygen species, toxicity, oxidative stress, and antioxidants: chronic diseases and aging [J]. Arch Toxicol, 2023, 97(10): 2499-2574.
- [21] LYU Y J, MENG Z P, HU Y Y, et al. Mechanisms of mitophagy and oxidative stress in cerebral ischemia-reperfusion, vascular dementia, and Alzheimer's disease[J]. Front Mol Neurosci, 2024, 17: 1394932.
- [22] HE F, RU X L, WEN T. NRF2, a transcription factor for stress response and beyond[J]. Int J Mol Sci, 2020, 21(13): 4777.
- [23] YANG S X, XIE Z P, PEI T T, et al. Salidroside attenuates neuronal ferroptosis by activating the Nrf2/HO1 signaling pathway in $A\beta_{1-42}$ -induced Alzheimer's disease mice and glutamate-injured HT22 cells[J]. Chin Med, 2022, 17(1): 82.
- [24] 黄 健, 曹诗杰, 安红伟. 自噬与血管性痴呆关系研究进展[J]. 中华老年心脑血管病杂志, 2022, 24(2): 219-221.
- [25] WEI P H, JIA M, KONG X Y, et al. Human umbilical cord-derived mesenchymal stem cells ameliorate perioperative neurocognitive disorder by inhibiting inflammatory responses and activating BDNF/TrkB/CREB signaling pathway in aged mice[J]. Stem Cell Res Ther, 2023, 14(1): 263.
- [26] KAISAR M A, VILLALBA H, PRASAD S, et al. Offsetting the impact of smoking and e-cigarette vaping on the cerebrovascular system and stroke injury: Is Metformin a viable countermeasure? [J]. Redox Biol, 2017, 13: 353-362.
- [27] GEORGE M, THARAKAN M, CULBERSON J, et al. Role of Nrf2 in aging, Alzheimer's and other neurodegenerative diseases[J]. Ageing Res Rev, 2022, 82: 101756.